Volume 15 No.2
Juli 2023
ISSN : 2085 – 1669
e-ISSN : 2460 – 0288
Website : jurnal.umj.ac.id/index.php/jurtek
Email : jurnalteknologi@umj.ac.id

Jurnal Teknologi
UNIVERSITAS MUHAMMADIYAH JAKARTA

HYDRODYNAMICS ANALYSIS OF JANUS SPHERE AT VARIATIONS OF THE REYNOLDS NUMBER

James Julian[1*], Waridho Iskandar[1], Fitri Wahyuni[1]
[1]Mechanical Engineering, Faculty of Engineering, Universitas Pembangunan Nasional Veteran Jakarta, 12450, Indonesia
*Email: zames@upnvj.ac.id

Diterima: 28 Maret 2023 Direvisi: 14 Mei 2023 Disetujui: 28 Juli 2023

ABSTRAK

Hidrodinamika dari homogen sphere dan juga Janus sphere dibandingkan secara komputasional pada berbegai variasi bilangan Reynolds. Janus sphere terbagi menjadi dua bgian yaitu slippery dimana diatur sebagai wall free-slip dan sticky yang diatur sebagai wall free-slip. Persamaan yang digunakan merupkan persamaan RANS pada aliran fluida laminar. Penelitian lebih berfokus pada gaya hidrodinamika dan viasulisasi aliran fluida dengan menggunakan kontur dan streamline kecepatan. Domain dari proses komputasi diatur dalam bentuk persegi panjang. Mesh diverifikasi dengan metode Ricahrdson Extrapolation dan memberikan hasil bahwa variasi mesh berada dalam rentang konvergensi. Mesh dengan jumlah elemen 10^5 digunakan untuk proses komputasi lebih lanjut karena hanya memberikan error terendah sebesar 0.129%. Sementara itu hasil validasi menunjukkan bahwa proses komputasi dapat mengikuti hasil eksperimen pada $0°\leq\theta\leq80°$. Janus sphere secara hidrodinamika lebih baik jika dibandingkan dengan homogen sphere dimana C_l yang dihasilkan lebih besar dan C_d yang dihasilkan lebih kecil. Janus sphere dapat mencegah separasi pada bilangan Reynolds 20 dan dapat memperkecil area resirkulasi pada bilangan Reynolds 50.

Kata kunci: *free-slip, hidrodinamika, homogen sphere, Janus sphere, no-slip*

ABSTRACT

The hydrodynamics of the homogeneous and Janus spheres were compared computationally at various Reynolds number variations. The Janus sphere is divided into two parts: slippery, which is set as a free-slip wall, and sticky, which is arranged as a free-slip wall. The equation used is the RANS equation for laminar fluid flow. Research focuses more on hydrodynamic forces and visualization of fluid flow by using velocity contours and streamlines. The domains of computational processes are arranged in a rectangular shape. The Richardson Extrapolation method verifies the mesh and gives the result that the meh variation is within the convergence range. Mesh with 10^5 elements is used for further computation because it only gives the lowest error of 0.129%. Meanwhile, the validation results show that the computational process can follow the experimental results at $0°\leq\theta\leq80°$. The Janus sphere is hydrodynamically better than the homogeneous sphere, where the C_l produced is larger and the C_d produced is smaller. The Janus sphere can prevent separation at a Reynolds number of 20 and reduce the recirculation area at a Reynolds number of 50.

***Keywords**:free-slip, hydrodynamics, homogen sphere, Janus sphere, no-slip*

DOI: https://dx.doi.org/10.24853/jurtek.15.2.315-324

ISSN : 2085 – 1669
e-ISSN : 2460 – 0288

INTRODUCTION

There are many types of flow implementations on spherical geometry objects. It can be found in industrial applications such as fluidized bed reactors, spray drying, and bubble column reactors. Research on spherical geometry has been carried out quite a lot. Among them is the hydrodynamic and hydrodynamic characterization of the spherical geometry. In general, the geometry used is spherical with a homogeneous surface. There is various important information regarding hydrodynamic and hydrodynamic capacities on a homogeneous spherical geometry. However, one type of spherical geometry is rarely studied, namely heterogeneous spherical. This heterogeneous spherical is commonly known as the Janus sphere. The Janus sphere is generally defined as a heterogeneous particle with slippery and sticky surfaces. Because it has a different surface, all the behaviors of the Janus sphere are automatically very different compared to homogeneous spherical objects. The Janus sphere has extensive uses, including bubble column reactors, mineral processing, and fluidized bed reactors. Thus, research on the Janus sphere can majorly contribute to various industrial applications. Currently, the Janus sphere manages migration and measures and studies cellular functions. Furthermore, the Janus sphere can also be applied in the biomedical field. The Janus sphere can be used to manipulate biological responses.

Although there are still very few studies studying the Janus sphere, several studies have been found which can become the foundations of science for future studies. One of the studies discussing the Janus sphere is Dhiman et al., who studied two Janus spheres positioned side by side. This study examines two cases. The first case is the Janus sphere, with the no-slip surfaces facing each other. This case is then referred to as case A. Meanwhile, the second case is the Janus sphere, with the free-slip surfaces facing each other. This case is then referred to as case B. Furthermore, there is also a discussion that analyzes the varied influence of the distance between the two Janus spheres. The research was conducted using the computational fluid dynamics (CFD) method. The fluid flow through the Janus sphere is assumed to be uniform. The results of this study concluded that the oscillations only occur on the back of the janus sphere, which has a no-slip surface. In case A, C_l is always positive for all distances between the spheres. The value of C_l will increase as the distance between the two spheres gets closer. Meanwhile, for case B the value of C_l can be positive or negative. However, C_l is negative at all distances if the Reynolds number is 20-50. The distance between the two Janus spheres has no significant effect on changes in C_d (Dhiman et al., 2021a). Narutomi et al. studied the three-dimensional flow of a spherical particle with a transient flow type. Particles are analyzed at low Reynolds numbers 30, 100, 200, and 250. The study results show that the drag force experienced by the particles is very dependent on the Reynolds number. In addition, the drag force on the particle is also very dependent on the distance from a particle to other particles. The drag force on the particles arranged streamwise becomes attenuated. The effect of the leading edge of the particle on the trailing edge of the particle is greater than the influence of the effect of the trailing edge of the particle on the leading edge of the particle. In the case of particles arranged side by side, the drag force generated by the two particles is augmented. Two factors can cause this condition. The first causative factor is the presence of coalescing and enlargement of the high-pressure area around the particles, thereby increasing the compressive drag value. Another factor is the increasing velocity gradient near the surface of the particle(Tsuji et al., 2003). Kotsev completed a computational study by studying the hydrodynamic effects of two or more rigid spherical particles on various types of arrangements. This study shows that the distance between particles dominates the fluid flow characteristics around the particles. One of the particle arrangements studied in this study is the particle arrangement with the V formation. In the V formation, the formation angle significantly affects the structure of the fluid flow oscillation behind the particles and the value of the drag force (Kotsev, 2018).

Through the paragraph above, quite a lot of research has been carried out on the hydrodynamics or hydrodynamics of sphere objects. However, these studies generally still discuss the homogeneous sphere. Research on the Janus sphere is still very rare. Even though there has been discussion about the Janus

sphere, this study only analyzed two Janus spheres arranged side by side. Research on the basic characteristics of the Janus sphere is still very rare. Thus, this study aims to analyze the fluid flow in the Janus sphere fundamentally and comprehensively. This research is expected to provide information regarding the hydrodynamic characteristics of the Janus sphere in order to complement the data differences regarding the Janus sphere. This study analyzes the hydrodynamic characteristics of the Janus sphere at various Reynolds number variations.

METODE PENELITIAN

Janus Sphere

The Janus sphere is a spherical particle consisting of two types of surfaces. In general, the two surfaces are proportionally divided, but in some cases, the two types of surfaces have an asymmetric area. In general, the surface of the Janus sphere consists of a slippery and sticky surface. The slippery surface has no-slip wall properties. This type of surface is a type of surface that is commonly found on a wall or surface (Dhiman et al., 2021b). The other surface is a sticky surface which is free-slip. In general, the illustration of the Janus sphere can be seen in Figure 1.

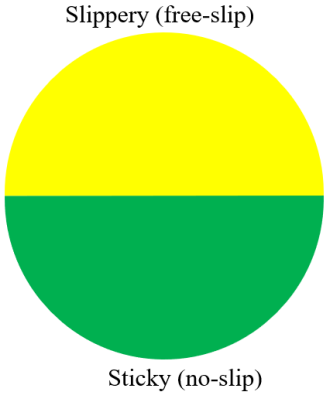

Figure 1. Janus sphere

No-slip Condition

The no-slip condition is the most common assumption for analyzing fluid flows moving through a wall. No slip occurs when a fluid moves on a wall or vice versa with the condition that the velocity of the fluid particles on the wall's surface is zero. The friction between the fluid particles and the interacting walls causes this. Furthermore, the farther a fluid particle is from the wall surface, the smaller the friction value experienced by the particle. The consequence of this phenomenon is that the velocity of the fluid will be more incredible the farther it is from the wall. However, this only occurs within a boundary layer. When the fluid flow is outside the boundary layer, it will be more inviscid, and friction is considered non-existent. The shape of the velocity profile of the no-slip wall condition is in the form of a Blasius curve, as shown in Figure 2 (Neto et al., 2003).

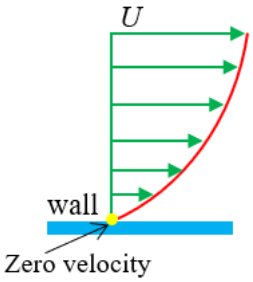

Figure 2. Velocity profile at wall no-slip

Free-slip Condition

The free-slip condition is when the fluid has a uniform velocity at any distance from the wall. In other words, in the free slip condition, the distance variable between the wall and the fluid does not affect each other. This condition is also known as the inviscid condition. Generally, the free slip condition can be found in falling droplets when the droplet surface interacts with the airflow. The free slip condition is very rarely found in solid objects. However, a fluid flow through a solid body can sometimes be assumed as a free-slip condition. Some examples are fluid flow on a smooth and slippery glass surface. In addition, the airflow through the hot air balloon can also be considered a free-slip condition because the material from the hot air balloon is slippery and smooth. The fluid flow velocity profile in the free-slip condition can be seen in Figure 3 (Cerquaglia et al., 2017).

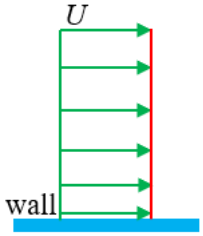

Figure 3. Velocity profile at free-slip

ISSN : 2085 – 1669
e-ISSN : 2460 – 0288

Drag Forces

Drag force is an important aspect that must be considered in the hydrodynamic and hydrodynamic analysis of the Janus sphere. The drag force can affect the Janus sphere's movement both around air fluids or other types of Newtonian fluids (Julian and Karim, 2017)(Harinaldi et al., 2015). Drag force is a force that inhibits the movement of an object (Julian et al., 2016a). Therefore, the direction of the drag force is always opposite to the direction of motion of an object (Iskandar et al., 2022)(Julian et al., 2016b). Several factors, including the fluid velocity or the speed of movement of an object, the fluid's density, and the object's size and shape, influence the drag force (Julian et al., 2018)(Harinaldi et al., 2016). In this study, the drag force is given as a coefficient. The equation to calculate the drag force coefficient can be seen in Equation 1 (Julian et al., 2022a)(Kosasih et al., 2019).

$$C_d = \frac{2d}{\rho UD} \quad (1)$$

whereas,

C_d : coefficient of drag
d : drag force
ρ : density of fluid
D : diameter of sphere
U : Free-stream flow

Lift Forces

The lift force is one of the forces that is highly considered in the hydrodynamic analysis is the lift force. This force acts in a direction perpendicular to the free stream (Megawanto et al., 2019). This force can be generated by manipulating the velocity of the fluid flowing over an object so that it has a higher velocity than the velocity of the fluid flowing at the bottom of the object or object (Megawanto et al., 2018). The consequence of this event is that the pressure at the bottom becomes greater when compared to the pressure at the top (Harinaldi et al., 2020)(Harinaldi et al., 2019). It is an application of Bernoullie's principle. The lift force equation is given in equation 2 (Julian et al., 2022b).

$$C_l = \frac{2l}{\rho UD} \quad (2)$$

whereas,

C_l : coefficient of lift
l : drag force

Computation Setup

The computational process is carried out with various considerations to obtain satisfactory results (Julian et al., 2023). The governing equation used is the RANS equation, as used by Julian et al (Julian et al., 2022c). Meanwhile, because the fluid is considered a laminar flow, no turbulence model is used and only uses the Laminar equation (Harinaldi et al., 2019). The type of fluid used for computational processes is water liquid under normal conditions. The geometry used in the computational process consists of a rectangle with dimensions 200 times the diameter of the sphere and 140 times the sphere's diameter. It is done to eliminate the influence of boundary conditions on the simulation results. The dimensions of the geometry can be seen in Figure 4. The boundary conditions for this study are velocity-inlet for the inlet channel and pressure outlet for the fluid exit. Meanwhile, the wall area above and below the sphere is considered the boundary condition symmetry. The Janus sphere consists wall (no-slip) and a wall with zero friction.

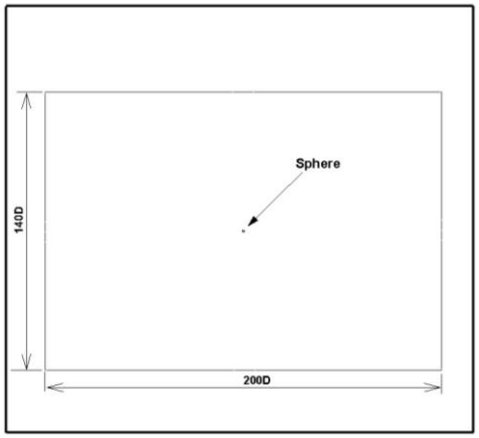

Figure 4. Computation setup

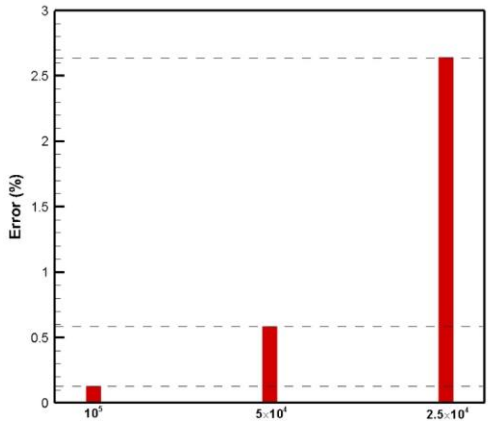

Figure 5. Error of each mesh

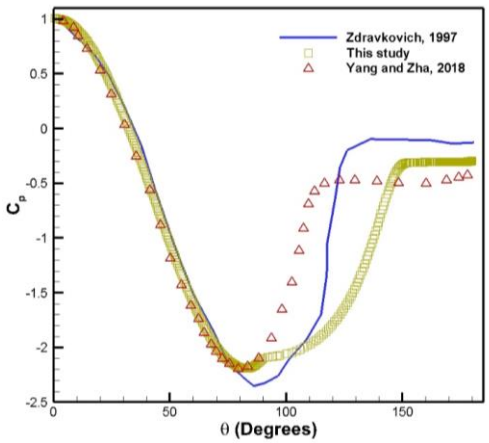

Figure 6. Computation validation

RESULTS AND DISCUSSION

The mesh independence test in this study is a stage known as verification. This stage is necessary to ensure that the mesh used is feasible for the computational process. Using a variation of three meshes distinguished by the number of mesh elements, the first variation is a mesh with 10^5 elements, while the second variation is 5×10^4 and the third is 2.5×10^4. The Reynolds number used for this verification step is 50 in a homogeneous sphere. The data is extracted at coordinates x=0 and y=0.0007, where at this position the fluid flow is disturbed due to the presence of spheres resulting in flow fluctuations. Each stage of the mesh independence test is carried out sequentially according to research conducted by Julian et al (Julian et al., 2022d). The results of the verification are given in Figure 5. This verification step obtained an error value of 0.129% for a 10^5 mesh, 0.584% for a mesh with 5×10^4 elements, and an error of 2.640% for a mesh with 2.5×10^4 elements. Thus, the computation process can be continued using a mesh with as many as 10^5 elements.

The results obtained from this study were then compared in a balanced manner to other studies with the same object and conditions. The comparison data used is the coefficient of pressure (C_p) data on the surface gap of the sphere. Because the sphere is symmetrical, the C_p data is only up to 180°. The Reynolds number used for this activity is a value of 10^6. As a comparison data, a research result was chosen experimentally by Zdravkovich, 1997 (Zdravkovich, 1977). This activity is referred to as the validation stage which is depicted in Figure 6. The results of the validation show that the data in this study show very good results where the data obtained is very close to the experimental data. However, the experimental and computational data agreement is limited to θ=80°. When θ>80°, the computational and experimental data show a significant difference (Yang and Zha, 2017). Other studies using computational methods also show the same results for this study, where the experimental data's compatibility is only up to θ=80°. It is due to the emergence of fluid flow separation. This fluid flow separation causes the fluid flow to be complex and difficult to predict by computational equations (Bao et al., 2020). Considering the results obtained from this activity, it can be concluded that the data obtained is valid enough, and research and data analysis can proceed to the next stage.

Furthermore, this study reveals hydrodynamic data from the Janus sphere. The hydrodynamic data given is in the form of hydrodynamic force coefficient data. This analysis is important to discover the things that cause the movement of the Janus sphere particles. Because the Janus sphere particles are very small, the Reynolds number used for research is a low Reynolds number. In this study, four variations of the Reynolds number were selected, namely 5, 10, 20, and 50. All the variations of the Reynolds number studied in this paper; the C_l produced by a consistent homogeneous sphere always had a value of 0. Very different results were obtained in the Janus sphere. The Janus sphere can produce a different increase in C_l values for each

ISSN : 2085 – 1669
e-ISSN : 2460 – 0288

variation of the Reynolds number. The greater the value of the Reynolds number, the greater the increase in the value of C_l in the Janus sphere. It is caused by the absence of a boundary layer which decreases velocity in the free slip area of the Janus sphere. Due to the curved shape of the Janus sphere, the fluid flow can be accelerated. The consequence of this is that there is a pressure drop on the surface. This concept can also be found in airfoils, where increased speed on the upper side reduces pressure in the same area. C_l of Janus sphere is given in Figure 7.

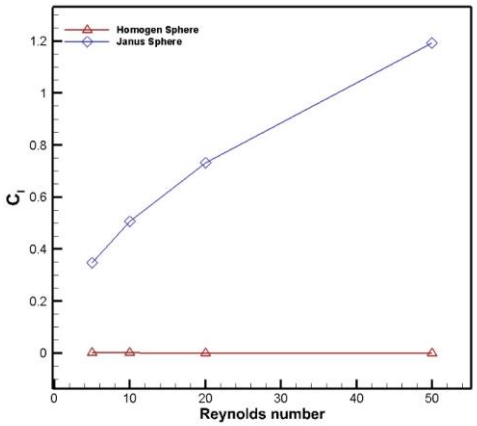

Figure 7. Comparion of C_l from Janus and homogen sphere

Furthermore, this study also compares the drag force coefficient (C_d) of the homogeneous sphere and the Janus sphere. The C_d data was released at the same variation of the Reynolds number as the C_l data. The drag force of the homogeneous sphere and the Janus sphere shows the same trend where an increase in the Reynolds number causes a decrease in the value of C_d as shown in Figure 8. Although it shows the same trend between homogeneous and Janus spheres, the resulting C_d values are very different for all variations of the Reynolds number. The Janus sphere is proven to have much lower C_d when compared to the homogeneous sphere. The cause of the decrease in C_d value will be analyzed further and comprehensively using fluid flow visualization, such as pressure contours and velocity contours. Apart from using fluid flow visualization in contours, the analysis is also deepened by using fluid flow visualization in the form of streamlined fluid flow velocity. Overall, from the point of view of hydrodynamic forces, it can be concluded that the Janus sphere has a much better performance when compared to the homogeneous sphere.

The velocity and pattern of fluid flow through the Janus Sphere are visualized using velocity contours and streamlines in Figure 9. Visualization was done on Reynolds numbers 5, 10, 20, and 50. On the Janus sphere, the contours are always different between the free-slip side and the no-slip side. It can be seen from all the variations of the Reynolds number studied. On the free-slip side, there is no decrease in the fluid flow velocity caused by friction between the free-slip surface and the fluid flow. It is caused by the absence of a boundary layer formed on the cylinder's surface, which reduces the fluid flow velocity within the boundary layer area. According to Benoullie's equation, high velocity is inversely proportional to pressure, so the pressure in the free-slip area is relatively low compared to the no-slip side. It is what causes the Janus Sphere to produce an lift force. From a streamlined viewpoint of fluid flow, there is no significant change between the homogeneous and Janus spheres. Meanwhile, at Reynolds numbers 20 and 50, there is a significant change in the streamline of fluid flow. At a Reynolds number of 20, the Janus sphere can prevent fluid flow separation. It can be seen from the loss of fluid flow recirculation. Meanwhile, at a Reynolds number of 50, recirculation of fluid flow still exists but can be reduced significantly.

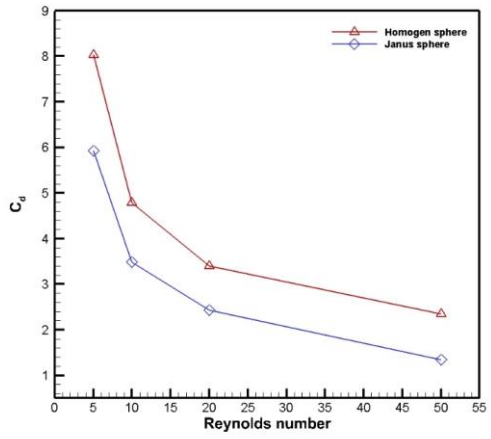

Figure 8. Comparion of C_d from Janus and homogen sphere

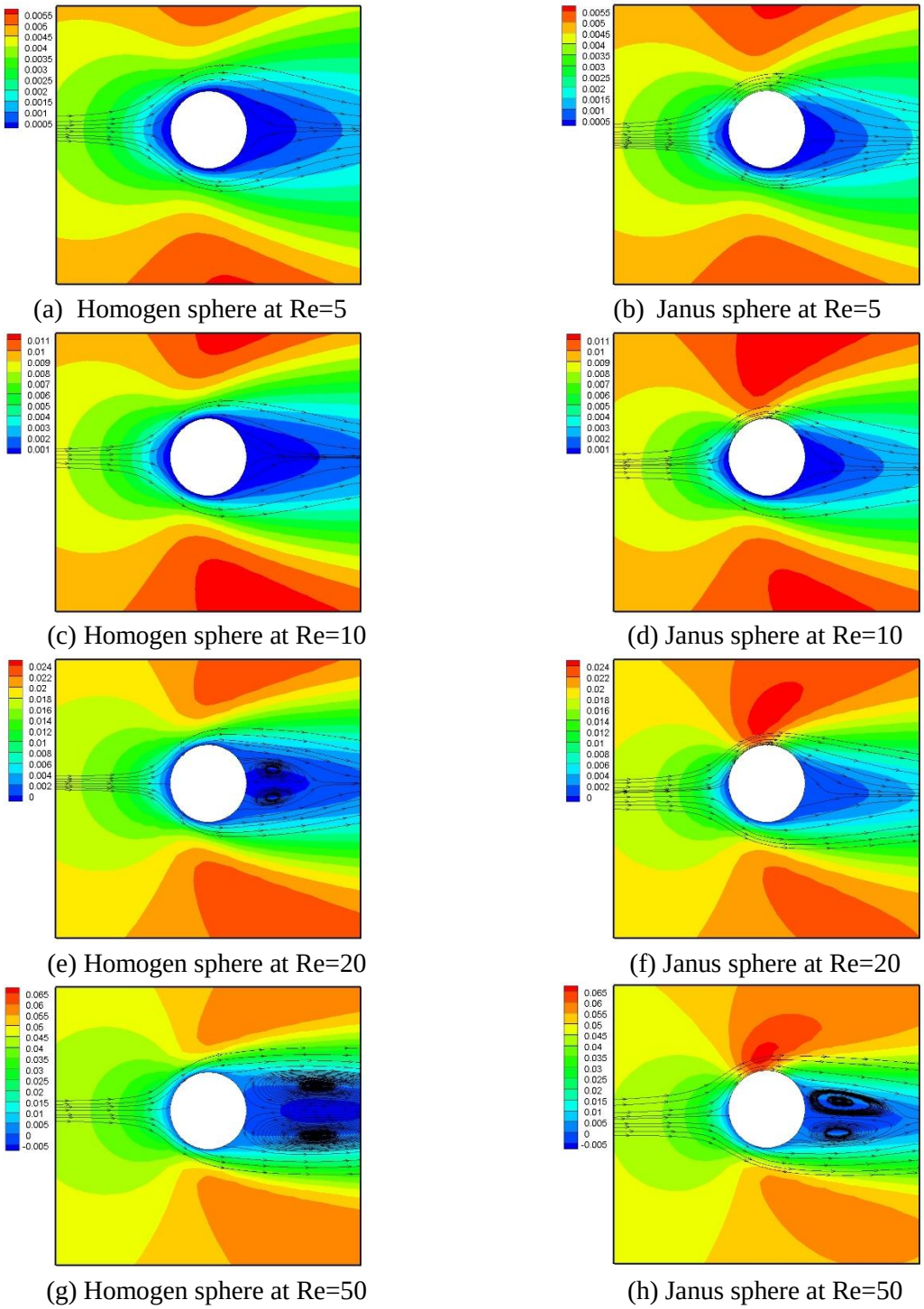

(a) Homogen sphere at Re=5 (b) Janus sphere at Re=5

(c) Homogen sphere at Re=10 (d) Janus sphere at Re=10

(e) Homogen sphere at Re=20 (f) Janus sphere at Re=20

(g) Homogen sphere at Re=50 (h) Janus sphere at Re=50

Figure 9. Velocity contour and streamline on Janus and homogen sphere

CONCLUSSION

This study discusses the hydrodynamics of the Janus sphere, which is analyzed using the CFD method. The Janus sphere in this study consisted of a free-slip wall at the top and a no-slip wall at the bottom. The study was conducted on four different variations of the Reynolds number, namely 5, 10, 20, and 50. The computational results were first validated using comparative data from experimental research. The results of the validation show that all computational settings have yielded fairly good results, where the computational and experimental results show similarities at θ=0° to θ=80°. Janus spheres show better hydrodynamic performance when compared to homogeneous spheres. It is evident from the value of C_l which has increased. In addition,

ISSN : 2085 – 1669
e-ISSN : 2460 – 0288

the C_d value of the Janus sphere also decreased significantly. Overall, the increase in C_l from the Janus sphere is caused by the free slip area experiencing lower pressure than the no-slip wall side. Furthermore, the Janus sphere can prevent the separation of fluid flows at a Reynolds number of 20. And can reduce the area of fluid flow separation at a Reynolds number of 50.

REFERENCES

Bao, H., Yang, W., Ma, D., Song, W., Song, B., 2020. *Numerical simulation of flapping airfoil with alula*. International Journal of Micro Air Vehicles 12.

Cerquaglia, M.L., Deliége, G., Boman, R., Terrapon, V., Ponthot, J.P., 2017. *Free-slip boundary conditions for simulating free-surface incompressible flows through the particle finite element method*. Int J Numer Methods Eng 110, 921–946.

Dhiman, M., Gupta, R., Reddy, K.A., 2021a. *Hydrodynamic interactions between two side-by-side Janus spheres*. European Journal of Mechanics, B/Fluids 87, 61–74.

Dhiman, M., Gupta, R., Reddy, K.A., 2021b. *Lift on Janus and stick spheres in laminar channel flow: a computational study*. Theor Comput Fluid Dyn 35, 659–682.

Harinaldi, Budiarso, Julian, J., 2016. *The effect of plasma actuator on the depreciation of the aerodynamic drag on box model*. In: AIP Conference Proceedings. AIP Publishing LLC, p. 040004.

Harinaldi, H., Budiarso, B., Julian, J., WS, A., 2015. *Drag Reduction in Flow Separation Using Plasma Actuator in a Cylinder Model*.

Harinaldi, Kesuma, M.D., Irwansyah, R., Julian, J., Satyadharma, A., 2020. *Flow control with multi-DBD plasma actuator on a delta wing*. Evergreen 7, 602–608.

Harinaldi, W., Adhika, S., Julian, J., 2019. *The comparison of an analytical, experimental, and simulation approach for the average induced velocity of a dielectric barrier discharge (DBD)*. In: The 10th International Meeting of Advances in Thermofluids (IMAT 2018): Smart City: Advances in Thermofluid Technology in Tropical Urban Development. p. 020027.

Iskandar, W., Julian, J., Wahyuni, F., Ferdyanto, F., Prabu, H.K., Yulia, F., 2022. *Study of Airfoil Characteristics on NACA 4415 with Reynolds Number Variations*. International Review on Modelling and Simulations (IREMOS) 15, 162.

Julian, J., Difitro, R., Stefan, P., 2016a. *The effect of plasma actuator placement on drag coefficient reduction of Ahmed body as an aerodynamic model*. International Journal of Technology 7, 306–313.

Julian, J., Harinaldi, Budiarso, Wang, C.-C., Chern, M.-J., 2018. *Effect of plasma actuator in boundary layer on flat plate model with turbulent promoter*. Proc Inst Mech Eng G J Aerosp Eng 232, 3001–3010.

Julian, J., Harinaldi, H., Budiarso, B., 2016b. THE EFFECT OF PLASMA ACTUATOR UTILIZATION TO THE REDUCTION OF AERODYNAMIC DRAG OF CYLINDER AND BOX MODELS.

Julian, J., Iskandar, W., Wahyuni, F., 2022a. *Aerodynamics Improvement of NACA 0015 by Using Co-Flow Jet*. International Journal of Marine Engineering Innovation and Research 7.

Julian, J., Iskandar, W., Wahyuni, F., 2022b. *Effect of Single Slat and Double Slat on Aerodynamic Performance of NACA 4415*, International Journal of Marine Engineering Innovation and Research.

Julian, J., Iskandar, W., Wahyuni, F., Bunga, N.T., 2022c. *Characterization of the Co-Flow Jet Effect as One of the Flow Control Devices*. Jurnal Asiimetrik:

Jurnal Ilmiah Rekayasa & Inovasi 185–192.

Julian, J., Iskandar, W., Wahyuni, F., Ferdyanto, F., 2022d. *COMPUTATIONAL FLUID DYNAMICS ANALYSIS BASED ON THE FLUID FLOW SEPARATION POINT ON THE UPPER SIDE OF THE NACA 0015 AIRFOIL WITH THE COEFFICIENT OF FRICTION*. Media Mesin: Majalah Teknik Mesin 23, 70–82.

Julian, J., Iskandar, W., Wahyuni, F., Nely Toding Bunga, dan, 2023. *Aerodynamic Performance Improvement on NACA 4415 Airfoil by Using Cavity* 5, 135–142.

Julian, J., Karim, R.F., 2017. *Flow control on a squareback model*. International Review of Aerospace Engineering 10, 230–239.

Karim, R.F., Julian, J., 2018. *Drag reduction due to recirculating bubble control using plasma actuator on a squareback model*. In: MATEC Web of Conferences. EDP Sciences, p. 01108.

Kosasih, E.A., Karim, R.F., Julian, J., 2019. *Drag reduction by combination of flow control using inlet disturbance body and plasma actuator on cylinder model*. Journal of Mechanical Engineering and Sciences 13, 4503–4511.

Kotsev, T., 2018. *Viscous flow around spherical particles in different arrangements*. In: MATEC Web of Conferences. EDP Sciences.

Megawanto, F.C., Harinaldi, Budiarso, Julian, J., 2018. *Numerical analysis of plasma actuator for drag reduction and lift enhancement on NACA 4415 airfoil*. In: AIP Conference Proceedings. AIP Publishing LLC, p. 050001.

Megawanto, F.C., Karim, R.F., Bunga, N.T., Julian, J., 2019. *Flow separation delay on NACA 4415 airfoil using plasma actuator effect*. International Review of Aerospace Engineering 12, 180–186.

Neto, C., Craig, V.S.J., Williams, D.R.M., 2003. *Evidence of shear-dependent boundary slip in newtonian liquids*. The European Physical Journal E 12, 71–74.

Tsuji, T., Narutomi, R., Yokomine, T., Ebara, S., Shimizu, A., 2003. *Unsteady three-dimensional simulation of interactions between flow and two particles*. International Journal of Multiphase Flow 29, 1431–1450.

Yang, Y., Zha, G., 2017. *Super-Lift Coefficient of Active Flow Control Airfoil: What is the Limit?* In: 55th AIAA Aerospace Sciences Meeting, AIAA SciTech Forum. American Institute of Aeronautics and Astronautics.

Zdravkovich, M.M., 1977. *REVIEW—Review of Flow Interference Between Two Circular Cylinders in Various Arrangements*. J Fluids Eng 99, 618–633.

ISSN : 2085 – 1669
e-ISSN : 2460 – 0288